

Photophysical Properties of Ternary RE³⁺ (RE = Eu, Tb, Sm) Hybrids with β -Diketone Functionalized Linkages and 4-(4-nitrostyryl)pyridine Through Coordination Bonding

Yan-Yan Li · Bing Yan · Lei Guo

Received: 31 July 2011 / Accepted: 18 October 2011 / Published online: 29 October 2011
© Springer Science+Business Media, LLC 2011

Abstract In this paper, the organic ligands TTA and TAA are grafted onto the coupling agent to achieve the organic precursors (TTA-Si, TAA-Si) as first ligand and the organic 4-(4-nitrostyryl)pyridine (Nspy) is synthesized as the second ligand. Both of them are coordinated to the rare ions with the carbonyl group and nitrogen atom respectively. After the hydrolysis and copolycondensation between the tetraethoxysilane (TEOS) and the ternary rare earth organic complex via the sol–gel process, the chemical bonded hybrid materials are constructed and characterized in detail. The obtained hybrid materials present superior thermal stabilities and regular and homogenous square blocks microstructure. Among the hybrids Eu(TTA-Si)₃Nspy shows a more strong characteristic emission and longer lifetime than the hybrids Eu(TAA-Si)₃Nspy, while hybrids Tb(TAA-Si)₃Nspy exhibits the stronger characteristic emission and longer lifetime than the hybrids Tb(TTA-Si)₃Nspy. For Sm³⁺ hybrid materials, the photoluminescence of Sm(TAA-Si)₃Nspy is too weak to find in the characteristic emission spectra, meanwhile, Sm(TTA-Si)₃Nspy has the excellent luminescent intensity.

Keywords Rare earth ion · Hybrid materials · Luminescence · Photophysical property

Introduction

The rare earth based organic–inorganic hybrid materials have a wide variety of potential applications such as fluorescent

biology, dyestuff, fluoroimmunoassays [1, 2], magnetic resonance imaging (MRI), NIR-emitting probes and amplifiers for optical communications [3–7]. A number of investigations on the hybrid materials have been done in the past decade. Generally speaking, the conventional physical doping hybrid systems seem to be easily to occur the quenching effect of the luminescent centers, leach of the photoactive molecules and cluster of the emitting center because of the weak interactions between the interfaces and the high energy vibration by the surrounding hydroxyl groups [8]. Therefore, in recent years, many studies have focused their attention on the encapsulation of luminescent rare earth complexes in silica-based matrices via strong covalent bond, where the organic ligands can absorb the enough energy and transfer it to the emitting metal to sensitize them [9–11]. Moreover, embedding a rare earth complex in an inorganic matrix via the strong covalent bond in the process of sol–gel is beneficial for its thermal stability, mechanic properties and luminescence output. More recently, Binnemans has reviewed extensive research progress in the field of rare earth-based luminescent hybrid systems [12]. In view of the researches, the key procedure to construct molecular-based materials is to design the “functional bridge molecule” which could be obtained by the grafting reaction, where it can both coordinates lanthanide ions and constitutes the covalent Si–O network [8, 13–18].

In this paper, we select TTA and TAA as the organic ligands, and they have been modified by the addition of the 3-(triethoxysilyl) propyl isocyanate (TEPIC) and obtained the bridge molecules TTA-Si and TAA-Si. The 4-(4-nitrostyryl) pyridine (Nspy) has been synthesized. We take the bridge molecule as the organic ligand and the Nspy as the second ligand to construct the better luminescent hybrid systems. In these hybrid systems, the bridge molecule and Nspy can coordinate to the RE³⁺ by the carbonyl groups

Y.-Y. Li · B. Yan (✉) · L. Guo
Department of Chemistry, Tongji University,
Siping Road 1239,
Shanghai 200092, China
e-mail: byan@tongji.edu.cn

and nitrogen atom respectively, the Si–O network is formed after the cohydrolysis and copolycondensation processes between the bridge molecule and the tetraethoxysilane (TEOS) [19–24]. The characteristics of the resulting materials are analyzed and compared in details. Through the comparison of the different organic ligands, it is recognized that TTA is more favorable to sensitize the photoluminescence of the Eu^{3+} materials and Sm^{3+} materials than TAA, while TAA is more benefit to sensitize the luminescent of the Tb^{3+} materials than TTA.

Experiment Section

Materials $\text{Ln}(\text{NO}_3)_3$ ($\text{Ln} = \text{Eu}, \text{Tb}, \text{Sm}$) are obtained by dissolving their respective oxides (Eu_2O_3 , Tb_4O_7 and Sm_2O_3) in concentrated nitric acid. 2-Thenoyltrifluoroacetone (TTA) and trifluoroacetylacetone (TAA) are purchased from the Aladdin, Tetraethoxysilane (TEOS) is distilled and stored under a N_2 atmosphere, 3-(triethoxysilyl)-propyl isocyanate (TEPIC) is purchased from Lancaster Synthesis Ltd, The solvent tetra-hydrofuran (THF) is used after desiccation with anhydrous calcium chloride, All the reagents are analytically pure, Other starting reagents are used as received.

Measurements

The ultraviolet spectroscopy is measured by the Agilent 8453 spectrophotometer at the room temperature. The FT-IR spectra are obtained on the Nexus 912 AO446 FT-IR spectrophotometer with KBr pellet as the blank, in the range of $4,000\text{--}400\text{ cm}^{-1}$. We obtain the ultraviolet–visible diffuse reflection spectra of the powder samples on the BWS003 spectrophotometer. ^1H NMR spectra are recorded in deuterate DMSO by a Bruker AVANCE-500 spectrometer with tetramethylsilane (TMS) as internal reference. Scanning electronic microstructure (SEM) are also used to give a comprehensive description of the hybrid materials morphology on Philip XL30 at the room temperature. The luminescent excitation and emission spectra are obtained on a RF spectrophotometer. The luminescent decay properties are recorded on an Edinburgh Analytical Instruments.

Synthesis

Synthesis of Precursor TTA-Si and TAA-Si

Following the literature procedure [19–25], the bridge molecules TTA-Si and the TAA-Si are acquired. Firstly, TTA (2 mmol, 0.444 g) is dissolved in 20 mL of dehydrate THF and NaH is added into the solution with stirring, 2 h

later the TEPIC (4 mmol, 0.990 g) is then put into the refluxing solution by drops. Then, the mixture is heated at $65\text{ }^\circ\text{C}$ and refluxed in a covered flask for 12 h at the nitrogen atmosphere, finally, a yellow oiled liquid is furnished after isolation and purification and characterized by IR and NMR. IR: $-(\text{CH}_2)_3-$ $2,975\text{ cm}^{-1}$, Si–O $1,167\text{ cm}^{-1}$, $-\text{CONH}-$ $1,628\text{ cm}^{-1}$. Anal. Calcd. For $\text{C}_{25}\text{H}_{47}\text{O}_{10}\text{N}_2\text{F}_3\text{Si}_2$ (648.82): C, 46.28; H, 7.30; N, 4.32. Found: C, 45.93; H, 7.04; N, 4.09%. ^1H NMR (CDCl_3): δ 0.64 (4H, t), δ 1.26 (18H, t), δ 5.60 (2H, t), δ 6.97 (1H, d), δ 7.35 (1H, d), δ 7.51 (1H, d), δ 1.58 (4H, t), δ 3.12 (4H, t), δ 3.83 (12H, m). The synthesise procedure of bridge molecule TAA-Si is similar to that of TTA-Si except that the TTA is replaced by TAA. The precursor is characterized by IR and NMR. IR: $-\text{CONH}-$ $1,080\text{ cm}^{-1}$, Si–O $1,167\text{ cm}^{-1}$, $-(\text{CH}_2)_3-$ $2,976\text{ cm}^{-1}$. Anal. Calcd. For $\text{C}_{28}\text{H}_{47}\text{O}_{10}\text{F}_3\text{N}_2\text{Si}_2\text{S}$ (716.92): C, 46.91; H, 6.60; N, 3.91. Found: C, 47.08; H, 6.46; N, 3.73%. ^1H NMR (CDCl_3): δ 0.62 (4H, t), δ 1.23 (18H, t), δ 3.14 (4H, m), δ 3.75 (12H, q), δ 4.75 (2H, t), δ 1.61 (4H, m), δ 1.89 (3H, s). From the IR and ^1H NMR dates of the bridge molecules TTA-Si and TAA-Si, it is demonstrated that the TEPIC has grafted onto the ligand TTA and TAA.

Synthesis of 4-(4-Nitrostyryl) Pyridine (Nspy)

Nspy is prepared according to the procedure reported in previous literature [26] as following: 4-picoline (0.186 g, 2 mmol) and 4-nitrobenzaldehyde (0.302 g, 2 mmol) are dissolved in a round bottom flask with 20 mL acetic anhydride as solvent. The mixture is heated at $90\text{ }^\circ\text{C}$ in a covered flak and refluxed for approximately 18 h. After isolation and recrystallization, the desired product is obtained. IR: cis-C=C $1,762\text{ cm}^{-1}$, anti-C=C 969 cm^{-1} ; $-\text{CH}-$ $3,019\text{ cm}^{-1}$. Anal. Calcd. For $\text{C}_{13}\text{H}_{10}\text{O}_2\text{N}_2$: ^1H NMR (CDCl_3): δ 7.13 (1H, d), δ 7.32 (1H, d), δ 8.62 (2H, br d), δ 8.16–8.22 (2H, m), δ 7.60–7.65 (2H, m), δ 7.38–7.42 (2H, m).

Synthesis of the Finally Hybrid Systems

The sol–gel-derived hybrid material is prepared as follows: The organic cross-linking precursor TTA-Si is dissolved in N, N-dimethylformamide (DMF) solvent, then $\text{RE}(\text{NO}_3)_3$ and Nspy are dropwise added into the solution under stirring respectively. The mixed solution is agitated magnetically for several hours at room temperature, after the coordination reaction had completed between the organic precursor TTA-Si, the secondary organic Nspy and $\text{RE}(\text{NO}_3)_3$. Then, an approximately TEOS, HCl and H_2O are put into the mixed solution by drops. The mixed solution is continued agitated magnetically for approximately 18 h to obtain a single phase in a covered Teflon beaker. After that, it is aged at $65\text{ }^\circ\text{C}$ until the onset of gelation in about 6 days. The gels ware denoted as $\text{RE}(\text{TTA-Si})_3\text{Nspy}$ and are ground into powdered

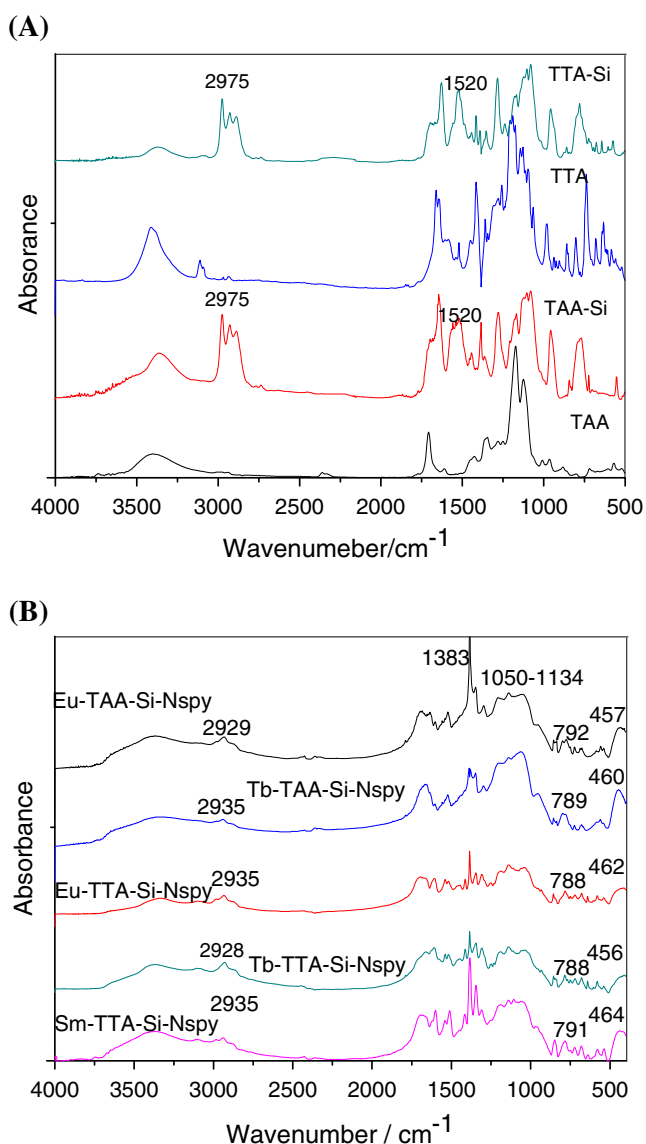


Fig. 2 FTIR spectra of **a** beta-diketones and linkages; **b** the hybrid systems: Eu(TTA-Si)₃Nspy, Eu(TAA-Si)₃Nspy, Tb(TTA-Si)₃Nspy, Tb(TAA-Si)₃Nspy, Sm(TTA-Si)₃Nspy

the UV-visible diffuse reflection spectrum is very similar to the excitation of the Eu³⁺ hybrid systems.

The excitation and emission spectra of the resulting europium hybrid materials are shown in Fig. 4a and b. A high baseline is observed in the emission spectra of Eu(TAA-Si)₃Nspy, which indicates the energy transfer efficiency between TAA and Eu³⁺ is low, while for Eu(TTA-Si)₃Nspy, the base line is very low. The emission lines of hybrid material Eu(TTA-Si)₃Nspy are assigned to ⁵D₀→⁷F_J transitions located at around 576, 587, 613, 648, and 695 nm, for J=0, 1, 2, 3, and 4, respectively, while in hybrid Eu(TAA-Si)₃Nspy, only ⁵D₀→⁷F_J (J=0, 1, 2) transitions at 576, 587 and 613 nm are obtained, the ⁵D₀→⁷F₀ and ⁵D₀→⁷F₄ transitions are too weak to be

clearly seen from the emission spectra of the sample. Meanwhile, we can see that the emission intensities of these two kinds of materials are determined in orders: Eu(TTA-Si)₃Nspy > Eu(TAA-Si)₃Nspy, which may be explained by energy transfer degree. In addition, among the emission peaks of these hybrid systems, the electronic dipole transition ⁵D₀→⁷F₂ located at 613 nm is the strongest emission, which indicates that the chemical environment of Eu³⁺ is in low symmetry because the electronic dipole transition ⁵D₀→⁷F₂ strongly varies with the local symmetry of Eu³⁺, while the magnetic dipole transition ⁵D₀→⁷F₁ which is very independent of the environment of Eu³⁺ is much weaker than the electronic dipole transition. Furthermore, we can also see that the intensities ratio of red emission to orange emission is large which can also indicate that the Eu³⁺ is in an anti-symmetric environment

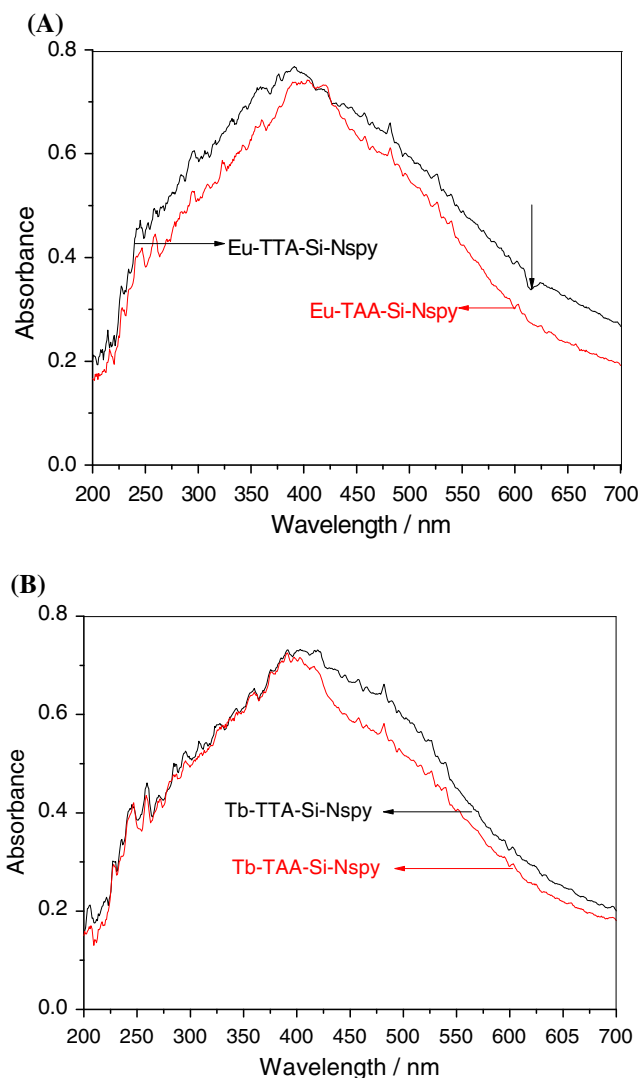


Fig. 3 Ultraviolet-visible diffuse reflection absorption spectra of **a** Eu(TTA-Si)₃Nspy and Eu(TAA-Si)₃Nspy; **b** Tb(TTA-Si)₃Nspy and Tb(TAA-Si)₃Nspy

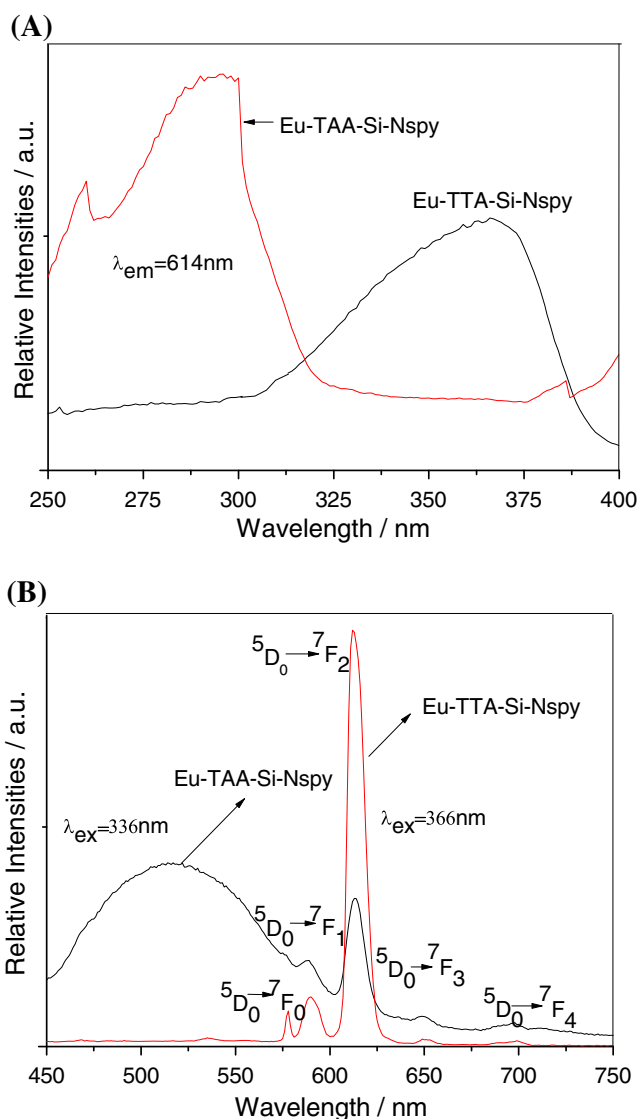


Fig. 4 Excitation spectra (a) and emission spectra (b) of europium hybrids (Eu(TTA-Si)₃Nspy, Eu(TAA-Si)₃Nspy)

[29]. A prominent feature that may be noted in these spectra is the low intensity ratios of $I(^5D_0 \rightarrow ^7F_2)/I(^5D_0 \rightarrow ^7F_1)$. The intensity (the integration of the luminescence band) ratio of the $^5D_0 \rightarrow ^7F_2$ transition to $^5D_0 \rightarrow ^7F_1$ transition has been widely used as an indicator of Eu^{3+} site symmetry [30]. When the interactions of the rare-earth complex with its local chemical environment are stronger, the complex becomes more nonsymmetrical and the intensity of the electric-dipolar transitions becomes more intense. As a result, $^5D_0 \rightarrow ^7F_1$ transition (magnetic-dipolar transitions) decreased and $^5D_0 \rightarrow ^7F_2$ transition (electric-dipolar transitions) increased. In this situation, the intensity ratios are approximately 2.3 which mean that the matrix didn't disturb the coordination between the organic groups and lanthanide ions.

The luminescence properties of Tb(TTA-Si)₃Nspy and Tb(TAA-Si)₃Nspy are shown in Fig. 5a and b respectively. The

emission lines assigned to the $^5D_4 \rightarrow ^7F_J$ transitions are located at 490, 543, and 586 nm, for J=6, 5, and 4 respectively. Among all these emission peaks, the most striking green luminescence ($^5D_4 \rightarrow ^7F_5$) is observed due to the fact that this emission is the most intense one in the emission spectra. Besides, the more smooth baseline of the characteristic emission of the Tb(TAA-Si)₃Nspy indicates the more effective energy transfer between the ligand TTA-Si and the Rare earth ion, compared to that of Tb(TTA-Si)₃Nspy. What have discussed in the front may indicate that the TTA may be more favorable for the luminescence of the Tb^{3+} , which may be explained by the energy degree. Of course, other factors such as relatively rigid structure of silica gel which can limit the vibration of ligand of Tb^{3+} and prohibit nonradiative transitions may also contribute to the striking green emission.

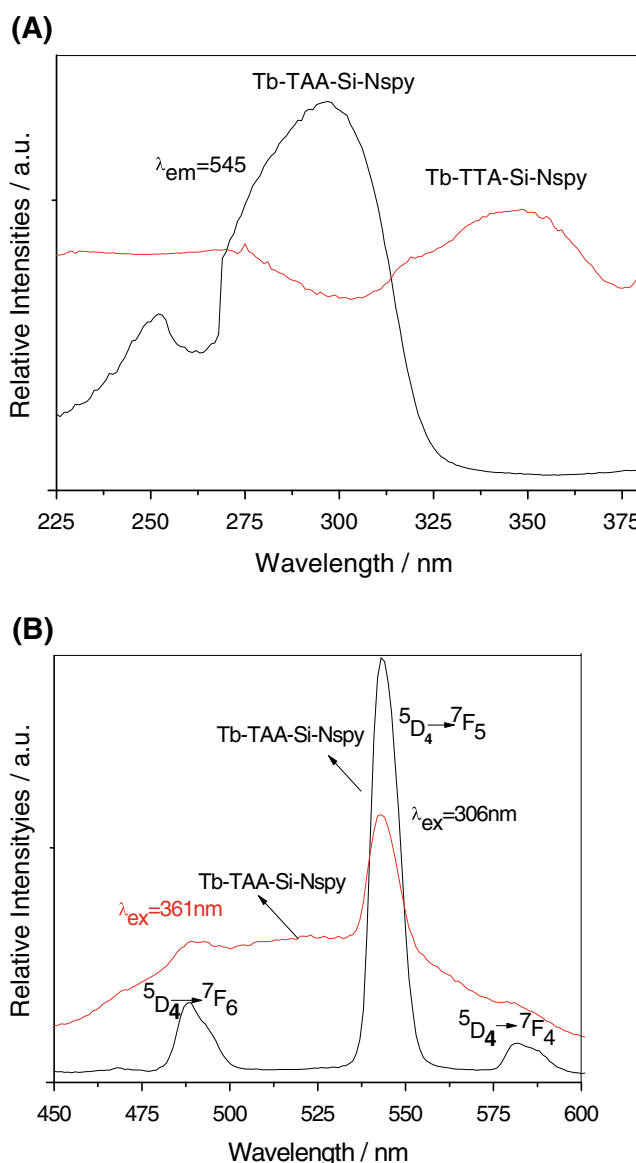


Fig. 5 Excitation spectra (a) and emission spectra (b) of terbium hybrids (Tb(TTA-Si)₃Nspy, Tb(TAA-Si)₃Nspy)

For $\text{Sm}(\text{TTA-Si})_3\text{Nspy}$ hybrid material, a broad excitation band centered at around 367 nm is observed in Fig. 6a. With the 367 nm as the excitation wavelength, the peaks at 560 nm, 595 nm, and 644 nm assigned to the ${}^4\text{G}_{5/2} \rightarrow {}^6\text{H}_J$ transitions for $J=5/2, 7/2,$ and $9/2$ respectively are viewed in Fig. 6b and the most intense emission is located at 644 nm. Moreover, a broad emission band is observed which indicates that the ligand TTA has not effectively transferred the energy to the Sm^{3+} . The low energy transfer efficiency may be prevented by selecting the energy-matching ligand. While for $\text{Sm}(\text{TAA-Si})_3\text{Nspy}$, the intensities of its emission spectra are so weak that cannot be seen from the emission spectra. Accordingly, we may also expect that through this efficient way, the leaching of the photoactive molecules and

clustering of the emitting could be avoided and a better photoluminescence of hybrid material is obtained.

The emission quantum efficiency (η) of the ${}^5\text{D}_0$ excited state can be determined on the basis of the emission spectrum and the lifetime of the Eu^{3+} firstly excited level ($\tau, {}^5\text{D}_0$). Assuming that only nonradiative and radiative processes are essentially involved in the depopulation of the ${}^5\text{D}_0$ state, the experimental luminescence lifetime can be calculated by the equation [31–37].

$$\tau_{\text{exp}} = (A_r + A_{\text{nr}})^{-1} \quad (1)$$

The A_r and A_{nr} represent the radiative transition rates and nonradiative transition rates respectively. The quantum efficiency of the luminescence, which can be defined as the possession ratio of the radiative transition to the total transition, is calculated by the following equation.

$$\eta = A_r / (A_r + A_{\text{nr}}) \quad (2)$$

According to the Eqs. 1 and 2, the η which can be described as the product of the radiative transition and the luminescence decay time, the equation as the followed.

$$\eta = A_r \tau_{\text{exp}} \quad (3)$$

Here, A_r is achieved by summing over the radiative rates A_{0J} for each ${}^5\text{D}_0 \rightarrow {}^7\text{F}_J$ transitions of Eu^{3+} .

$$A_r = \sum A_{0J} = A_{00} + A_{01} + A_{02} + A_{03} + A_{04} \quad (4)$$

Considering the magnetic dipole ${}^5\text{D}_0 \rightarrow {}^7\text{F}_1$ transition is independent of Eu^{3+} chemical environment, so it is available as the internal reference for the whole spectrum. The other experimental coefficients of spontaneous emission, A_{0J} can be calculated according to the equation.

$$A_{0J} = A_{01} (I_{0J}/I_{01}) (\nu_{01}/\nu_{0J}) \quad (5)$$

In this equation, A_{0J} is the experimental coefficients of spontaneous emission, where J is representative for 0, 1, 2, 3 and 4 respectively. The ${}^5\text{D}_0 \rightarrow {}^7\text{F}_5$ and ${}^5\text{D}_0 \rightarrow {}^7\text{F}_6$ can be neglected for the truth that their influence can be ignored in the depopulation of the ${}^5\text{D}_0$ excited state. The A_{01} is the Einstein's coefficient of spontaneous emission of the ${}^5\text{D}_0 \rightarrow {}^7\text{F}_1$. In vacuum, the value of A_{01} can be determined

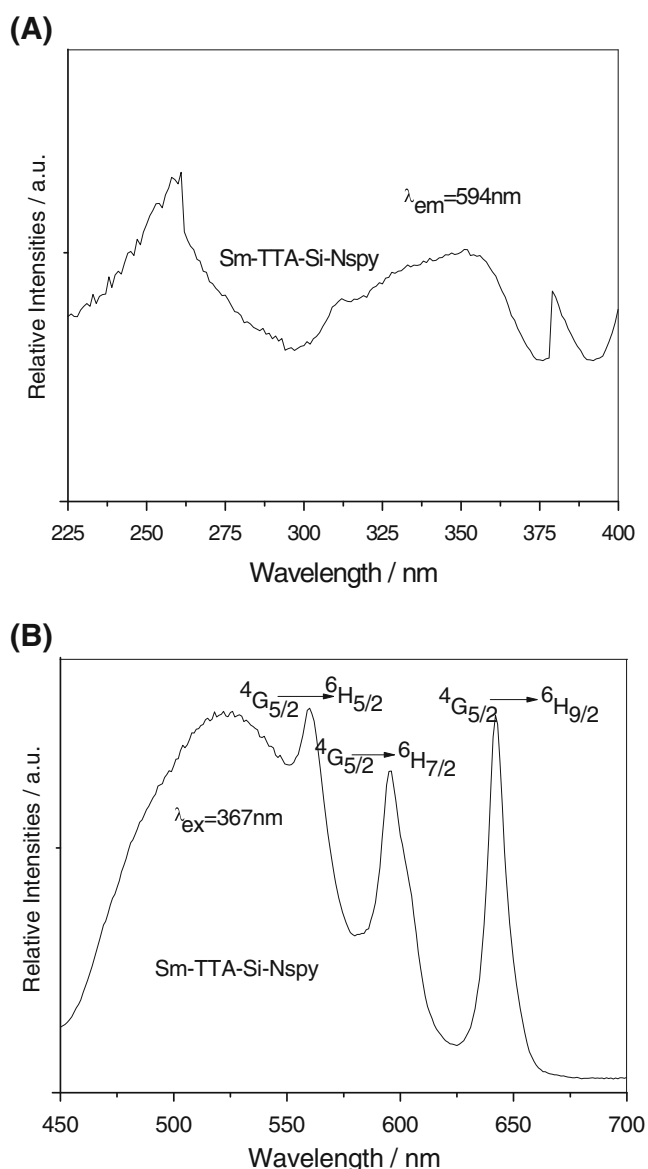


Fig. 6 Excitation and emission spectra (a) and (b) of samarium hybrids ($\text{Sm}(\text{TTA-Si})_3\text{Nspy}$)

Table 1 Luminescence decay times (τ) and emission quantum efficiency (η)

System	Eu-TTA-Si-Nspy	Eu-TAA-Si-Nspy
τ (μs) ^a	426	355
A_{rad} (s^{-1})	505	288
η (%)	22	11
I_{02}/I_{01}	6.25	4.5

^a The luminescence decay times of ${}^5\text{D}_0 \rightarrow {}^7\text{F}_2$ transitions

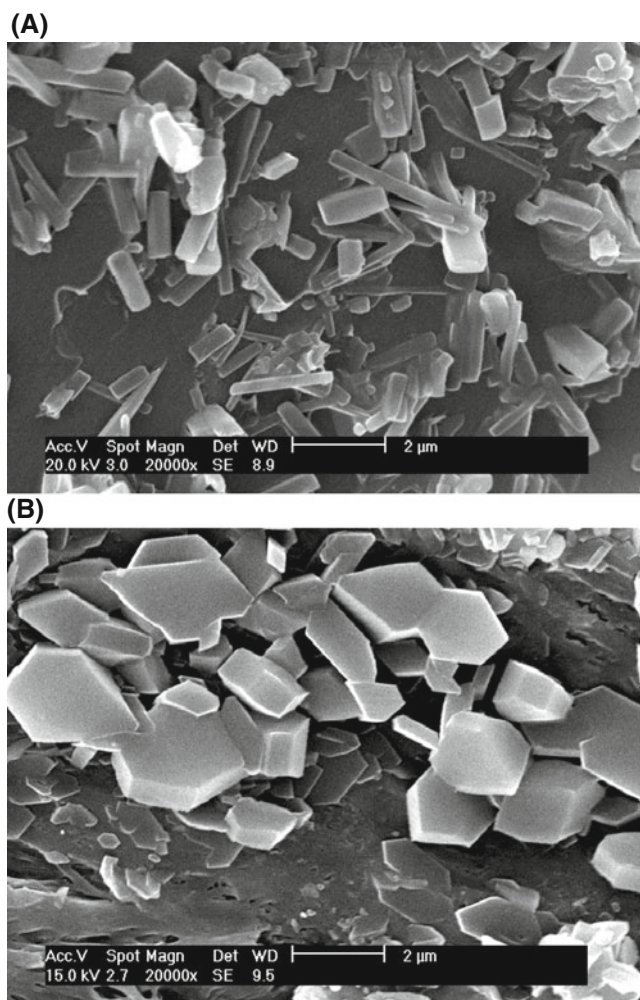


Fig. 7 Scanning electron micrographs of **a** Eu(TTA-Si)₃Nspy; **b** Tb(TAA-Si)₃Nspy

to be 50 s^{-1} approximately ($A_{01} = n^3 A_{01}(\text{vacuum})$). [32, 35], I is the emission intensity which can be taken as the integrated intensity of the ${}^5\text{D}_0 \rightarrow {}^7\text{F}_J$ emission bands [36, 37], ν_{0J} refers to the energy barycenter and can be determined from the emission bands of Eu^{3+} 's ${}^5\text{D}_0 \rightarrow {}^7\text{F}_J$ emission transitions. According to the above discussion, it can be seen there are two mainly factors contributing to the value η , one factor is lifetime and the other is I_{02}/I_{01} (red/orange ratio). If the lifetimes and red/orange ratio are both large, the quantum efficiency must be high. The quantum efficiencies of the two kinds of europium hybrid systems are described in Table 1, it can be seen in this order Eu-TTA-Si-Nspy > Eu-TAA-Si-Nspy. The conclusion can be drawn that the organic ligand TTA is more favorable for luminescence of the Eu^{3+} hybrid material than the organic ligand TAA.

The scanning electron micrographs of the hybrid materials demonstrate that the homogeneous, molecular-based materials are obtained. Compared with the physical

doping hybrid materials which generally experience the phase separation phenomena, in this paper the inorganic and organic phases can exhibit their distinct properties together in the hybrid materials containing covalent bonds [38]. The selected scanning electron micrographs of systems are shown in the Fig. 7a and b respectively. The micrograph of Eu(TTA-Si)₃Nspy is made up of a lot of single, ordered rectangular parallelepiped (see Fig. 7a) which indicate the regular, homogeneous hybrid material has been obtained. Meanwhile, the micrograph of Tb(TAA-Si)₃Nspy is made up of a great deal of regular square blocks (see Fig. 7b). Considering the ligand TTA or TAA has the multidimensional β -diketone with the thiophene ring or a methylic, two carbonyl groups, and a trifluoromethyl group, so its derivative TTA-Si or TAA-Si is prone to form a two-dimensional layer-like or three-dimensional network-like microstructure, and its corresponding complex may also keep this trend. So this regular three-dimensional structure we obtained may be due to the fact that the specific β -diketone ligand acts as a functional bridge combining inorganic matrices and organic components together.

Conclusions

In summary, the covalent linkage (TTA-Si or TAA-Si) is obtained and the organic Nspy is synthesized, which are both used to assemble the ternary rare earth (Eu^{3+} , Tb^{3+} , Sm^{3+}) hybrid system. The homogeneous microstructures and morphologies of these hybrid systems show the occurrence of self-assembly between the inorganic network and organic chain. Besides, the luminescence properties of these systems indicate that the ternary systems have a longer time and higher quantum efficiency than the binary systems. Moreover, we can see that the hybrids Eu(TTA-Si)₃Nspy shows a better luminescence than the hybrids Eu(TAA-Si)₃Nspy. While the hybrids Tb(TAA-Si)₃Nspy exhibits a better luminescence than the hybrids Tb(TTA-Si)₃Nspy. In addition, the hybrids Sm(TTA-Si)₃Nspy presents apparent photoluminescence of Sm^{3+} , while the hybrids Sm(TAA-Si)₃Nspy does not.

Acknowledgments This work is supported by the National Natural Science Foundation of China (20971100) and program for New Century Excellent Talents in University (NCET-08-0398).

References

1. Elbanowshi M, Makowska B (1996) The lanthanides as luminescent probes in investigations of biochemical systems. *J Photochem Photobiol A Chem* 99:85
2. Kido J, Okamoto Y (2002) Organo lanthanide metal complexes for electroluminescent materials. *Chem Rev* 102:2357

3. Escribano P, Lopez BJ, Arago JP, Cordoncillo E, Viana B, Sanchez CJ (2008) Photonic and nanobiophotonic properties of luminescent lanthanide-doped hybrid organic–inorganic materials. *J Mater Chem* 18:23
4. Carlos LD, Ferreira RAS, Bermudez VDZ, Ribeiro SJL (2009) Lanthanide-containing light-emitting organic–inorganic hybrids: a bet on the future. *Adv Mater* 21:509
5. Le Quang AQ, Zyss J, Ledoux I, Truong VG, Jurdy AM, Jacquier B, Le DH, Gibaud A (2005) An hybrid organic–inorganic approach to erbium-functionalized nanodots for emission in the telecom window. *Chem Phys* 318:33
6. Que WX, Hu X (2007) Optical switch and luminescence properties of sol–gel hybrid organic–inorganic materials containing azobenzene groups and doped with neodymium ions. *Appl Phys B* 88:557
7. Caravan P, Ellison JJ, McMurry TJ, Lauffer RB (1999) Gadolinium(III) chelates as MRI contrast agents: structure, dynamics, and applications. *Chem Rev* 99:2293
8. Yan B, Lu HF (2008) Lanthanide-centered covalently bonded hybrids through sulfide linkage: molecular assembly, physical characterization, and photoluminescence. *Inorg Chem* 47:5601
9. Sabbatini N, Guardingli M, Lehn JM (1993) Luminescence of Eu^{3+} and Tb^{3+} complexes of a novel branched macrocyclic ligand containing 2,2'-bipyridine and 9-methyl-1,10-phenanthroline subunits. *Coord Chem Rev* 123:201
10. Reisfeld R (2004) Rare earth ions: their spectroscopy of cryptates and related complexes in glasses. *Struct Bond* 106:209
11. de Sa GF, Malta OL, Donega CD, Simas AM, Longo RL, Santa-Cruz PA, da Silva EF (2000) Spectroscopic properties and design of highly luminescent lanthanide coordination complexes. *Coord Chem Rev* 196:165
12. Binnemans K (2009) Lanthanide-based luminescent hybrid materials. *Chem Rev* 109:4283
13. Wang QM, Yan B (2004) Novel luminescent terbium molecular-based hybrids with modified meta-aminobenzoic acid covalently bonded with silica. *J Mater Chem* 14:2450
14. Yan B, Qian K, Lu HF (2007) Molecular assembly and photophysical properties of quaternary molecular hybrid materials with chemical bond. *Photochem Photobiol* 83:1481
15. Liu JL, Yan B (2008) Lanthanide (Eu^{3+} , Tb^{3+}) centered hybrid materials using modified functional bridge chemical bonded with silica: molecular design, physical characterization, and photophysical properties. *J Phys Chem B* 112:10898
16. Yan B, Wang QM (2008) Two luminescent molecular hybrids composed of bridged Eu(III)-beta-diketone chelates covalently trapped in silica and titanate gels. *Cryst Growth Des* 8:4184
17. Lu HF, Yan B (2006) Attractive sulfonamide bridging bonds constructing lanthanide centered photoactive covalent hybrids. *J Non-Cryst Solids* 352:5331
18. Yan B, Li YY, Guo L (2011) Photofunctional ternary rare earth (Eu^{3+} , Tb^{3+} , Sm^{3+}) hybrid xerogels with hexafluoroacetylacetonate derived building block and bis(2-methoxyethyl)ether through coordination bonds. *Inorg Chem Commun* 14:910
19. Yan B, Zhou B, Li Y (2009) Covalently bonding assembly and photophysical properties of luminescent molecular hybrids Eu-TTA-Si and Eu-TTASi-MCM-41 by modified thenoyltrifluoroacetone. *Microp Mesop Mater* 120:317
20. Li YJ, Yan B (2009) Lanthanide (Eu^{3+} , Tb^{3+})/beta-diketone modified mesoporous SBA-15/organic polymer hybrids: chemically bonded construction, physical characterization, and photophysical properties. *Inorg Chem* 48:8276
21. Yan B, Li Y (2010) Luminescent ternary inorganic-organic mesoporous hybrids Eu(TTASi-SBA-15)phen: covalent linkage in TTA directly functionalized SBA-15. *Dalton Trans* 39:1480
22. Li YJ, Yan B, Li Y (2010) Hybrid materials of SBA-16 functionalized by rare earth (Eu^{3+} , Tb^{3+}) complexes of modified beta-diketone (TTA and DBM): covalently bonding assembly and photophysical properties. *J Solid State Chem* 183:871
23. Li YJ, Yan B (2010) Photoactive europium(III) centered mesoporous hybrids with 2-thenoyltrifluoroacetone functionalized SBA-16 and organic polymers. *Dalton Trans* 39:2554
24. Wang C, Yan B, Liu JL, Guo L (2011) Photoactive europium hybrids of beta-diketone-modified polysilsesquioxane bridge linking Si-O-B(Ti)-O xerogels. *Eur J Inorg Chem*. doi:10.1002/ejic.201001069
25. Li YJ, Yan B, Li Y (2010) Luminescent lanthanide (Eu^{3+} , Tb^{3+}) ternary mesoporous hybrids with functionalized beta-diketones (TTA, DBM) covalently linking SBA-15 and 2,2'-bipyridine (bpy). *Microp Mesop Mater* 131:82
26. Lorange ED, Kramer WH, Gould IR (2002) Kinetics of reductive N–O bond fragmentation: the role of a conical intersection. *J Am Chem Soc* 124:15225
27. Qiao XF, Yan B (2009) Covalently bonded assembly of lanthanide/silicon-oxygen network/polyethylene glycol hybrid materials through functionalized 2-thenoyltrifluoroacetone linkage. *J Phys Chem B* 113:11865
28. Guo XM, Guo HD, Fu LS, Zhang HJ, Deng RP, Sun LN, Feng J, Dang S (2009) Novel hybrid periodic mesoporous organosilica material grafting with Tb complex: synthesis, characterization and photoluminescence property. *Microporous Mesoporous Mater* 119:252
29. Yan B, Wang C, Guo L, Liu JL (2010) Photophysical properties of Eu(III) center covalently immobilized in Si–O–B and Si–O–Ti composite gels. *Photochem Photobiol* 86:499
30. Wang Z, Wang J, Zhang HJ (2004) Luminescent sol–gel thin films based on europium-substituted heteropolytungstates. *Mater Chem Phys* 87:44
31. Malta OL, Couto dos Santos MA, Thompson LC, Ito NKJ (1996) Intensity parameters of 4f–4f transitions in the Eu(dipivaloyl-methanate)(3) 1,10-phenanthroline complex. *J Lumin* 69:77
32. Carlos LD, Messaddeq Y, Brito HF, Sa' Ferreira RA, Bermudez VD, Ribeiro SJL (2000) Full-color phosphors from europium(III)-based organosilicates. *Adv Mater* 12:594
33. Ferreira RAS, Carlos LD, Goncalves RR, Ribeiro SJL, Bermudez VD (2001) Energy-transfer mechanisms and emission quantum yields in Eu^{3+} -based siloxane-poly(oxyethylene) nanohybrids. *Chem Mater* 13:2991
34. Soares-Santos PCR, Nogueira HIS, Felix V, Drew MGB, Sa' Ferreira RA, Carlos LD, Trindade T (2003) Novel lanthanide luminescent materials based on complexes of 3-hydroxypicolinic acid and silica nanoparticles. *Chem Mater* 15:100
35. Teotonio EES, Espinola JGP, Brito HF, Malta OL, Oliveria SF, de Faria DLA, Izumi CMS (2002) Influence of the N-[methylpyridyl]acetamide ligands on the photoluminescent properties of Eu(III)-perchlorate complexes. *Polyhedron* 21:1837
36. Ribeiro SJL, Dahmouche K, Ribeiro CA, Santilli CV, Pulcinelli SHJ (1998) Study of hybrid silica-polyethyleneglycol xerogels by Eu^{3+} luminescence spectroscopy. *J Sol-Gel Sci Technol* 13:427
37. Werts MHV, Jukes RTF, Verhoeven JW (2002) The emission spectrum and the radiative lifetime of Eu^{3+} in luminescent lanthanide complexes. *Phys Chem Chem Phys* 4:1542
38. Ferreira RAS, Carlos LD, Goncalves RR, Ribeiro SGL, Bermudez VD (2001) Energy-transfer mechanisms and emission quantum yields in Eu^{3+} -based siloxane-poly(oxyethylene) nanohybrids. *Chem Mater* 13:2991